SAND2019-4288C

An Extension of Conditional Point Sampling to Quantify Uncertainty Due to Material Mixing Randomness

Emily H. Vu[1,2] **and Aaron J. Olson**[2]
[1]Department of Nuclear Engineering
University of California, Berkeley, CA 94720, USA

[2]Sandia National Laboratories
Albuquerque, NM 87185, USA

emilyhvu@berkeley.edu, aolson@sandia.gov

ABSTRACT

Radiation transport in stochastic media is a problem found in a multitude of applications, and the need for tools that are capable of thoroughly modeling this type of problem remains. A collection of approximate methods have been developed to produce accurate mean results but are not capable of quantifying the spread of those results caused by the randomness of material mixing. In this work, the new stochastic media transport algorithm Conditional Point Sampling is expanded using Embedded Variance Deconvolution such that it can compute the variance caused by material mixing. The accuracy of this approach is assessed for 1D, binary, Markovian-mixed media by comparing results to published benchmark values, and the behavior of the method is numerically studied as a function of user parameters. We demonstrate that this extension of Conditional Point Sampling is able to compute the variance caused by material mixing with accuracy dependent on the accuracy of the conditional probability function used.

KEYWORDS: Monte Carlo, Conditional Point Sampling, Parametric Variance, Embedded Variance Deconvolution, stochastic media

1. INTRODUCTION

For radiation transport problems in stochastic media, an accurate and efficient method that can be applied to multi-dimensional and multi-material geometries of arbitrary mixing types as well as characterize the spread of response mean results caused by random material mixing would be quintessential. Although several well-known approximate methods such as the atomic mix (AM) approximation and the Levermore-Pomraning (LP) closure, or its Monte Carlo equivalent Chord Length Sampling (CLS), have been demonstrated to produce mean results for this type of problem [1,2], there is not yet a method that can accurately compute parametric variance. Materials are homogenized in the AM approximation, such that there is no longer spread in random mixing to quantify. Chords of materials are sampled in CLS as the particle streams through the domain, but the memory of these materials is not retained during the lifetime of the particle. Although there are memory-enhanced versions of CLS (Algorithm A) [2], these methods are not able to calculate

the parametric variance because the realization is not preserved for more than one history. This preservation is required so that the total and Monte Carlo variances can each be computed.

Conditional Point Sampling (CoPS) uses Woodcock tracking [3] to stream particles to potential collision sites. The method assigns materials at pseudo-collision sites conditionally on previous material assignments using conditional probability functions while retaining full memory of the generated realization [4]. Using imperfect conditional probability functions is the only source of error since no bias error is introduced by the algorithm itself. We introduced CoPS in Ref. [4] and examined its accuracy in calculating mean leakage values using two derived conditional probability functions. We believe that in the special case of 1D, Markovian-mixed media, the second conditional probability function is errorless. In this paper, we use the same two conditional probability functions and focus on examining the use of CoPS to calculate estimations of the parametric variance in 1D. In a companion paper, we show that CoPS can extend accurately to multi-dimensional problems [5] and expect that the variance-computing method used here will straightforwardly port to multi-D.

To compute parametric variance, we implement Embedded Variance Deconvolution (EVADE) in CoPS, which was recently developed for computing this value. It requires that more than one particle history is simulated for a realization with full memory of sampled information [6]. We call this group of particles simulated per realization a cohort, and we call a group of cohorts a batch. Cohorts enable computation of the total and Monte Carlo variances. Batches enable computation of statistical uncertainty on these values. In this paper, the parametric variance results were produced using only two particle histories per realization in an effort to minimize error. Approximations are compounded in CoPS such that larger cohorts yield greater error leading to the hypothesis that error is minimized for the smallest useful cohort size: a size of two. We conduct numerical studies examining the error behavior as a function of history number in a cohort. The parametric variance values produced by the CoPS method using our 2-point and 3-point conditional probability functions are compared against the benchmark method results for the benchmark suites that were produced in Ref. [1].

2. PROBLEM DESCRIPTION

The stochastic transport equation of interest is

$$\mu\frac{\partial\psi(x,\mu,\omega)}{\partial x}+\Sigma_t(x,\omega)\psi(x,\mu,\omega)=\frac{\Sigma_s(x,\omega)}{2}\int_{-1}^{1}d\mu'\psi(x,\mu',\omega), \tag{1a}$$

$$0\leq x\leq L,-1\leq\mu\leq 1; \tag{1b}$$

$$\psi(0,\mu)=2,\mu\geq 0,\psi(L,\mu)=0,\mu<0, \tag{1c}$$

where x is the particle spatial variable, μ is the particle angular variable, and ω denotes the material realization. There is an isotropic boundary source with otherwise vacuum boundary conditions and a domain of length L.

Often, realizations of 1D, Markovian-mixed media are generated by successively sampling chord lengths starting at a boundary [1]. Here, we present the less-common method we will use in a later derivation, outlined in Ref. [7], which leverages the fact that the number of "pseudo-interfaces"

in a line randomly sampled from Markovian-mixed media is Poisson-distributed [8]. The average number of pseudo-interfaces per slab of length r is $I = \frac{r}{\Lambda_c}$, where Λ_C is the correlation length of the material and Λ_α and Λ_β are the average chord lengths in materials α and β [7]:

$$\Lambda_c = \frac{\Lambda_\alpha \Lambda_\beta}{\Lambda_\alpha + \Lambda_\beta}. \tag{2}$$

The frequency of k pseudo-interfaces is then

$$f(k, I) = e^{-I} \frac{I^k}{k!}. \tag{3}$$

This frequency is used to determine how many pseudo-interfaces are in a particular realization, and those pseudo-interfaces are distributed in the realization using a uniform distribition in space. The material in each cell defined by these pseudo-interfaces is then sampled independently according to the material abundances—unconditional probabilities—for each material. For binary media made up of materials α and β, as in this paper, the abundance of material α is computed as

$$P_\alpha = \frac{\Lambda_\alpha}{\Lambda_\alpha + \Lambda_\beta}. \tag{4}$$

3. CONDITIONAL POINT SAMPLING

Here, we present the Conditional Point Sampling (CoPS) algorithm as well as the 2-point (CoPS2) and 3-point (CoPS3) conditional probability functions that we derived in Ref. [4] for application with 1D, binary, Markovian-mixed media. Whereas the CoPS algorithm itself does not introduce error and is not tied to specific types of stochastic mixing, CoPS requires use of a material-mixing-specific conditional probability function that in all but special cases must be approximated. In the case of 1D, Markovian-mixed media, we believe our 3-point conditional probability function is errorless [4].

3.1. CoPS Algorithm

To begin Conditional Point Sampling, a particle history is initialized by setting the particle with a position x and direction μ. Distance to boundary, d_b, and distance to potential collision, $d_c^* = -\frac{1}{\Sigma_t^*} ln(\xi)$, where Σ_t^* is the majorant cross section and ξ is a randomly generated number, are sampled. The distance to the first event is chosen by taking the minimum of d_b and d_c^*. If the particle undergoes a potential collision, the collision is accepted with a probability equal to the ratio of the true and majorant total cross sections: $P_{col} = \frac{\Sigma_t}{\Sigma_t^*}$. Use of Woodcock tracking enables particles to stream to potential collisions without needing to know where materials or material boundaries are located. The following particle history flow summarizes the CoPS algorithm.

1. Initialize particle.
2. Sample the distance to potential collision, d_c^*, and distance to boundary, d_b.
3. Stream particle based on $min(d_c^*, d_b)$.
   (a) If the external boundary is crossed, terminate the particle.

(b) If the particle streams to a potential collision site, sample the material at that point conditionally on already defined points.

4. Sample if potential collision is accepted using P_{col}.
   (a) If the collision is accepted, evaluate collision.
   (b) If the collision is rejected, continue to stream particle by returning to step 2.

3.2. 2-Point Conditional Probability Function

Here, we derive the conditional probability of sampling material α at distance r from a point at which material α or β exists: $\pi(m = \alpha|\vec{m}, \vec{r})$. We compute the Poisson frequency of having no pseudo-interfaces between the new point and the nearest point and the complimentary frequency that there is at least one pseudo-interface. In the first scenario, the new point must have the same material type as the nearest point; in the second scenario, the material type is sampled according to the unconditional probability (i.e., material abundance). These likelihoods are combined in Eqs. (5) to derive the conditional probability of the new point being material α as a function of the distance to the nearest point and the material type of the nearest point:

$$\pi(m = \alpha|\vec{m} = \alpha, \vec{r} = r_1) = (1)f(k = 0, r = r_1) + (P_\alpha)f(k > 0, r = r_1), \tag{5a}$$

$$\pi(m = \alpha|\vec{m} = \beta, \vec{r} = r_1) = (0)f(k = 0, r = r_1) + (P_\alpha)f(k > 0, r = r_1). \tag{5b}$$

These reduce to

$$\pi(m = \alpha|\vec{m} = \alpha, \vec{r} = r_1) = 1 - \Big(1 - P_\alpha\Big)\Big(1 - e^{-\frac{r_1}{\Lambda_c}}\Big), \tag{6a}$$

$$\pi(m = \alpha|\vec{m} = \beta, \vec{r} = r_1) = P_\alpha\Big(1 - e^{-\frac{r_1}{\Lambda_c}}\Big). \tag{6b}$$

3.3. 3-Point Conditional Probability Function

The conditional probability of sampling material α for Markovian-mixed media for a new point when considering two points, one on each side, is denoted by $\pi(m = \alpha|\vec{m}, \vec{r})$, where $\vec{m}$ and $\vec{r}$ are vectors containing the corresponding material types and distances from each point: $\vec{m} = \{m_1, m_2\}$ and $\vec{r} = \{r_1, r_2\}$. Following the same logic as in the nearest-point derivation, the Poisson frequency of having no pseudo-interfaces or having at least one pseudo-interface between the new point and the points on each side are computed for the unique scenarios: α on each side, $\vec{m} = \{\alpha, \alpha\}$; β on each side, $\vec{m} = \{\beta, \beta\}$; and different materials on the sides, $\vec{m} = \{\alpha, \beta\}$. The scenario of having material α and material β on opposite sides of the new point and having zero pseudo-interfaces on both sides of the new point is unphysical and therefore invalid. This scenario does not therefore contribute to $\pi(m = \alpha|\{\alpha, \beta\}, \vec{r})$ and the probability contributions must be normalized by the likelihood of sampling a valid scenario (having at least one pseudo-interface).

$$\begin{aligned}\pi(m = \alpha|\{\alpha, \alpha\}, \vec{r}) = {} & (1)f(k = 0, r = r_1)f(k = 0, r = r_2) \\ & +(1)f(k > 0, r = r_1)f(k = 0, r = r_2) \\ & +(1)f(k = 0, r = r_1)f(k > 0, r = r_2) \\ & +(P_\alpha)f(k > 0, r = r_1)f(k > 0, r = r_2)\end{aligned} \tag{7a}$$

$$\begin{aligned}\pi(m=\alpha|\{\beta,\beta\},\vec{r}) = &(0)f(k=0,r=r_1)f(k=0,r=r_2)\\ &+(0)f(k>0,r=r_1)f(k=0,r=r_2)\\ &+(0)f(k=0,r=r_1)f(k>0,r=r_2)\\ &+(P_\alpha)f(k>0,r=r_1)f(k>0,r=r_2)\end{aligned} \tag{7b}$$

$$\begin{aligned}\pi(m=\alpha|\{\alpha,\beta\},\vec{r}) = &\frac{1}{f(k>0,r=r_1+r_2)}\times\\ &\Big[(0)f(k>0,r=r_1)f(k=0,r=r_2)\\ &+(1)f(k=0,r=r_1)f(k>0,r=r_2)\\ &+(P_\alpha)f(k>0,r=r_1)f(k>0,r=r_2)\Big]\end{aligned} \tag{7c}$$

These reduce to

$$\pi(m=\alpha|\{\alpha,\alpha\},\vec{r}) = 1-\Big(1-P_\alpha\Big)\Big(1-e^{-\frac{r_1}{\Lambda_c}}\Big)\Big(1-e^{-\frac{r_2}{\Lambda_c}}\Big), \tag{8a}$$

$$\pi(m=\alpha|\{\beta,\beta\},\vec{r}) = P_\alpha\Big(1-e^{-\frac{r_1}{\Lambda_c}}\Big)\Big(1-e^{-\frac{r_2}{\Lambda_c}}\Big), \tag{8b}$$

$$\pi(m=\alpha|\{\alpha,\beta\},\vec{r}) = \frac{1}{1-e^{-\frac{r_1+r_2}{\Lambda_c}}}\Big(1-e^{-\frac{r_2}{\Lambda_c}}\Big)\Big[1-\Big(1-P_\alpha\Big)\Big(1-e^{-\frac{r_1}{\Lambda_c}}\Big)\Big]. \tag{8c}$$

4. EMBEDDED VARIANCE DECONVOLUTION

To calculate parametric variance, we use the Embedded Variance Deconvolution (EVADE) approach [9]. This approach is an intrusive implementation for producing the parametric variance of a mean computed quantity when the Monte Carlo and parametric variance independently contribute to the total variance [9]. In EVADE, the total variance is computed using a history from each realization, the Monte Carlo variance is computed using more than one history per realization, and the parametric variance is the difference in these values. We introduce the concept of a cohort, which is a group of particle histories in CoPS that have memory of point-wise material designations made by each history in the cohort. In this way a cohort successively, but never fully, samples a realization. Batches of cohorts enable characterization of the uncertainty on these computed variances.

4.1. Statistical Calculations using Batches and Cohorts

The total variance is the sum of the Monte Carlo variance and the parametric variance as long as these these values are independent and normally distributed [6]. The parametric variance can therefore be computed by calculating each of these and taking the difference:

$$V_P = V_{tot} - V_{MC}. \tag{9}$$

The Monte Carlo (sample) variance of a quantity for each cohort i is estimated using

$$V_{MC_i} = \frac{N}{N-1}\left(\langle L^2\rangle_N - \langle L\rangle_N^2\right), \tag{10}$$

where L is a leakage quantity, N is the number of histories in the cohort, and moment p of L is estimated as

$$\langle L^p \rangle_N = \frac{1}{N} \sum_{n=1}^{N} L_n^p. \tag{11}$$

The average Monte Carlo variance for all possible realizations is then estimated as the average over the number of cohorts, R, in a batch:

$$V_{MC} = \frac{1}{R} \sum_{i=1}^{R} V_{MC_i}. \tag{12}$$

The total variance can be similarly calculated using one particle history from each of R cohorts:

$$V_{tot} = \frac{R}{R-1} \left(\langle L^2 \rangle_R - \langle L \rangle_R^2 \right). \tag{13}$$

We compute the statistical uncertainty on the computed parametric variance using B batches according to

$$U_P = \sqrt{\frac{1}{B-1} \left(\langle V_P^2 \rangle_B - \langle V_P \rangle_B^2 \right)}. \tag{14}$$

We use two histories per cohort to estimate the Monte Carlo variance and only the first history in each cohort for computing the mean results and estimating the total variance. Using only two histories per cohort maximizes the number of histories that contribute to the total variance [9] and we expect that it minimizes the uncertainty in the computed Monte Carlo variance in a way similar to that shown for the mean in Ref. [6]. In CoPS, error compounds as a function of the number of points defined, which is a function of the number of histories in a cohort. Therefore, using a small number of histories per cohort minimizes error in the computed Monte Carlo variance, and using the first history in the cohort minimizes the error in the computed mean and total variance. The relationships between error and cohort size and error and history number in the cohort are numerically examined later in this paper.

5. Results and Analysis

Ref. [1] provides a set of problem parameters for planar geometry from its benchmark suite. The problem parameters of Tables 10-18 in Ref. [1] are listed in Table 1, where $\Sigma_{t,j}$ is the total cross section, Λ_j is the average chord length, and c_j is the scattering ratio for each material $j \in \{0,1\}$. Only a slab length $L = 10$ is considered here.

In this paper, relative error is calculated using

$$E_R = \frac{x - x_{approx}}{x}, \tag{15}$$

where x is the benchmark value and x_{approx} is the value produced by the various implementations of CoPS. The statistical uncertainty of the relative error is propagated using

$$U_{E_R} = \sqrt{\left(\frac{U_{approx}}{x} \right)^2 + \left(\frac{x_{approx} U}{x^2} \right)^2}, \tag{16}$$

Table 1: Benchmark Set Parameters

Case Number	$\Sigma_{t,0}$	$\Sigma_{t,1}$	Λ_0	Λ_1	Case Letter	c_0	c_1
1	10/99	100/11	99/100	11/100	a	0.0	1.0
2	10/99	100/11	99/10	11/10	b	1.0	0.0
3	2/101	200/101	101/20	101/20	c	0.9	0.9

where x_{approx} and U_{approx} are the mean and statistical uncertainty of the approximate solver and x and U are the benchmark mean and statistical uncertainty values.

5.1. Leakage Results

In Table 2, the mean reflectance and transmittance results are provided for each case with a slab length of 10.0 for the benchmark approach (Bench) and the new implementation of CoPS using 2-point (CoPS2) and 3-point (CoPS3) probability functions. These benchmark values were generated in Ref. [4] using one history on each of 1E6 realizations and agree with values in Ref. [1]. The mean leakage results in Table 2 for CoPS2 and CoPS3 were produced using 1E6 particle histories and 40 batches with a cohort size of two particle histories, and the mean leakage values reported in the table were calculated by tallying the first particle history per cohort. These CoPS values agree within uncertainty with those produced without cohorts in Ref. [4]. Statistical uncertainties on the last digit are given in parentheses.

Figure 1 shows the relative error of CoPS2 and CoPS3 mean leakage results for each case. For the special case of 1D, binary, Markovian-mixed media, Figure 1 supports that CoPS3 has no bias error within uncertainty. CoPS2 results show error margins due to the fidelity of the conditional probability functions used.

5.2. Parametric Variance Results

Table 3 shows the reflectance and transmittance parametric variance results produced by Adams et al. in Ref. [1] as well as new CoPS2 and CoPS3 results. The CoPS2 and CoPS3 parametric variance results were generated along with the mean leakage results in Table 2 using 1E6 particle histories and 40 batches with two particle histories for each cohort. Since parametric variance is computed as the difference in the estimated total and Monte Carlo variances, a relatively small amount of bias error and/or statistical uncertainty may yield negative parametric variance estimates. This was the case for one computed value observed in Table 3 under the reflectance parametric variance for Case 2c using CoPS2.

The relative error of the parametric variance results produced for each case are shown in Figure 2. Similar to what was shown in Figure 1, Figure 2 shows that CoPS3 produces parametric variance with no bias error within uncertainty, whereas CoPS2 has bias error related to the fidelity of the conditional probability function used. We note that Case 1c values had large relative errors (plotted), but small absolute errors, possibly less than the uncertainty in the benchmark values.

Table 2: Reflectance and Transmittance Mean Results

Case	Reflectance			Transmittance		
	Bench [4]	CoPS2	CoPS3	Bench [4]	CoPS2	CoPS3
1a	0.4360(5)	0.4379(5)	0.4366(5)	0.0148(1)	0.0156(1)	0.0146(1)
1b	0.0850(2)	0.0716(3)	0.0852(3)	0.00166(4)	0.00141(4)	0.00161(3)
1c	0.4777(4)	0.4592(4)	0.4784(5)	0.0163(1)	0.0159(2)	0.0161(1)
2a	0.2372(4)	0.2438(5)	0.2366(6)	0.0980(2)	0.0974(3)	0.0986(3)
2b	0.2876(4)	0.2534(6)	0.2867(4)	0.1952(3)	0.1721(4)	0.1958(5)
2c	0.4326(4)	0.4174(5)	0.4343(5)	0.1870(3)	0.1807(4)	0.1866(4)
3a	0.6904(4)	0.6956(6)	0.6908(6)	0.1639(3)	0.1617(4)	0.1625(4)
3b	0.0363(1)	0.0292(2)	0.0358(2)	0.0762(2)	0.0628(3)	0.0751(4)
3c	0.4451(4)	0.4336(5)	0.4458(5)	0.1042(3)	0.0956(3)	0.1036(4)

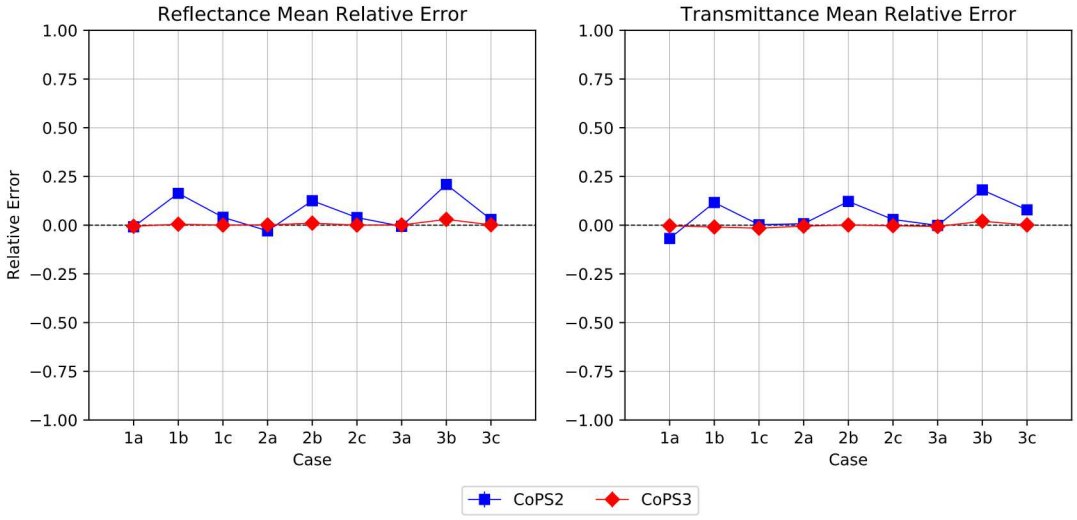

Figure 1: Reflectance and transmittance mean relative error and uncertainty for each case.

5.3. Effects of Cohort Size on Monte Carlo Variance Accuracy

Here, we investigate how the accuracy of the Monte Carlo variance behaves according to the number of particle histories in each cohort using a total of 1E6 particle histories and 40 batches on two benchmark problems. We use a cohort size of 2, 5, 10, and 25 particle histories to estimate the Monte Carlo variance and tally the first particle history in each cohort to the compute the total variance. Numerical results are shown in Table 4. Relative error is plotted in Figure 3. This approach holds the error in the total variance constant while increasing the error in the Monte Carlo variance. The overall error (and statistical uncertainty) increase as a function of cohort size.

Table 3: Reflectance and Transmittance Parametric Variance Results

Case	Reflectance			Transmittance		
	Bench [1]	CoPS2	CoPS3	Bench [1]	CoPS2	CoPS3
1a	0.02611	0.0246(3)	0.0264(4)	0.00023	0.0009(1)	0.0003(1)
1b	0.00486	0.0060(2)	0.0047(3)	0.00015	0.00027(4)	0.00012(4)
1c	0.00001	0.0001(5)	0.0006(3)	0.00038	0.0016(1)	0.0009(1)
2a	0.08180	0.0092(3)	0.0823(4)	0.00787	0.0092(3)	0.0079(3)
2b	0.02660	0.0274(5)	0.0261(4)	0.06508	0.0550(3)	0.0656(4)
2c	0.00327	-0.0006(3)	0.0030(3)	0.04554	0.0443(3)	0.0449(4)
3a	0.06838	0.0650(4)	0.0684(3)	0.03028	0.0302(3)	0.0308(3)
3b	0.00250	0.0037(2)	0.0030(2)	0.05072	0.0403(3)	0.0497(3)
3c	0.00852	0.0037(4)	0.0083(4)	0.05244	0.0476(3)	0.0527(3)

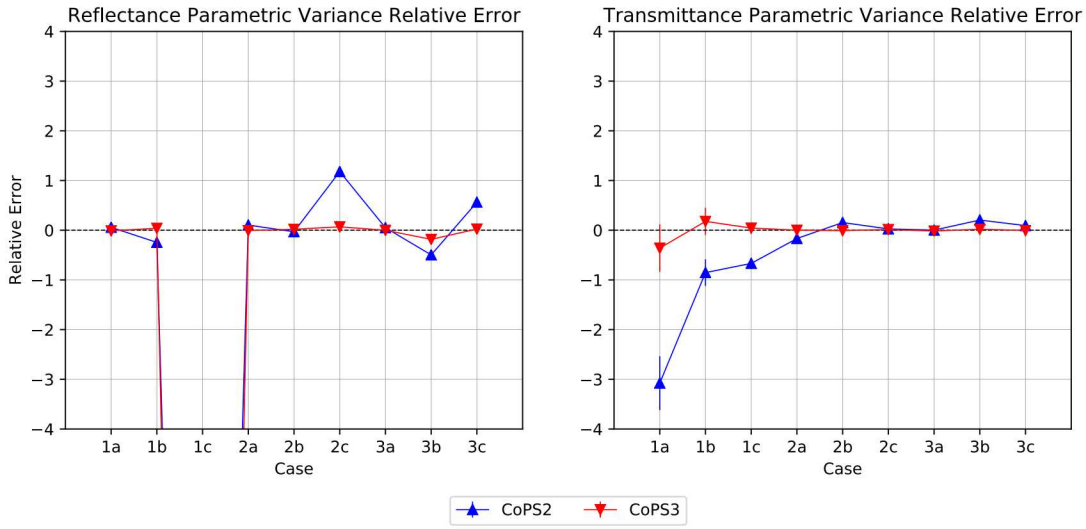

Figure 2: Reflectance and transmittance parametric variance relative error and uncertainty for each case.

5.4. Effects of Particle Index on Mean and Total Variance Accuracy

Here, we investigate how the accuracy of the mean and total variance behave according to the particle histories' order in a realization. We tallied particles 1, 2, 5, 10, or 25 in each cohort to calculate mean and parametric variance values using 1E6 particle histories with 25 particles for each cohort and 40 batches for Cases 2b and 3a. Numerical results are provided in Table 5 and error is plotted in Figure 4. This approach holds the error in the Monte Carlo variance constant (yielded by a cohort size of 25) while increasing the error in the mean and total variance computations.

Table 4: Reflectance and Transmittance Parametric Variance Results of Cohort Size

Case	Leakage	Cohort Size			
		2	5	10	25
2b	Ref.	0.0274(4)	0.0297(4)	0.0329(6)	0.0340(9)
	Trans.	0.0550(3)	0.0658(5)	0.0716(7)	0.075(1)
3a	Ref.	0.0640(4)	0.0624(4)	0.0592(5)	0.0596(8)
	Trans.	0.0302(3)	0.0347(5)	0.0359(8)	0.039(1)

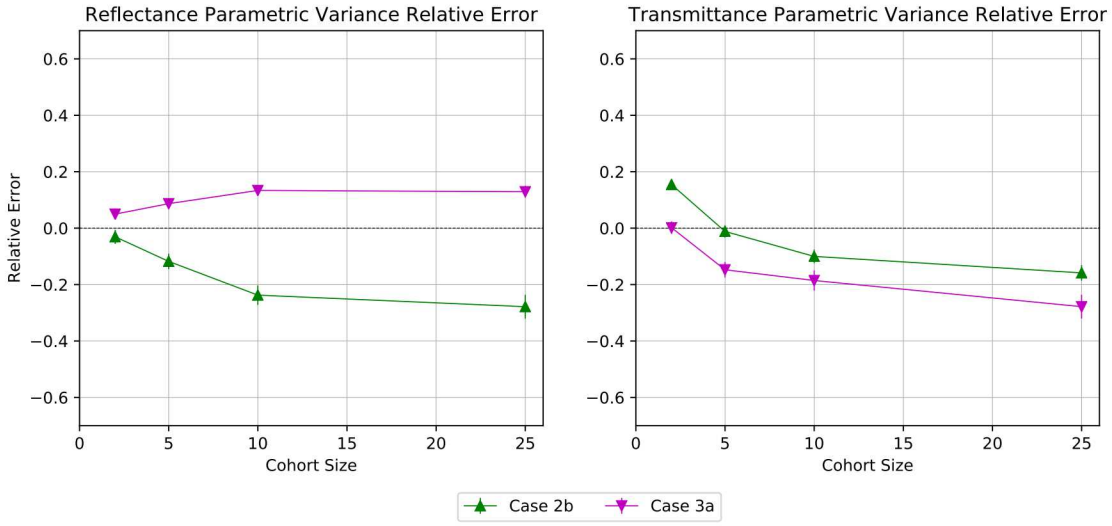

Figure 3: Reflectance and transmittance parametric variance relative error and uncertainty based on cohort size for Cases 2b and 3a.

Because material points are defined conditionally on neighboring material points, error is compounded as a function of number of material points defined. When many points are defined in a cohort, a realization is mostly sampled and error compounding slows resulting in an error plateau. Figure 4 captures the behavior of the mean and total variance estimates based on which history in each cohort is tallied for Cases 2b and 3a. The mean and parametric variance values shown in Table 5 were benchmarked against mean leakage results produced in Ref. [4] and variance results produced in Ref. [1].

6. CONCLUSIONS

Embedded Variance Deconvolution (EVADE) was implemented in Conditional Point Sampling (CoPS) enabling CoPS to compute parametric variance. The accuracy of this method was assessed using a 2-point and a 3-point conditional probability function on a set of binary Markovian-mixed

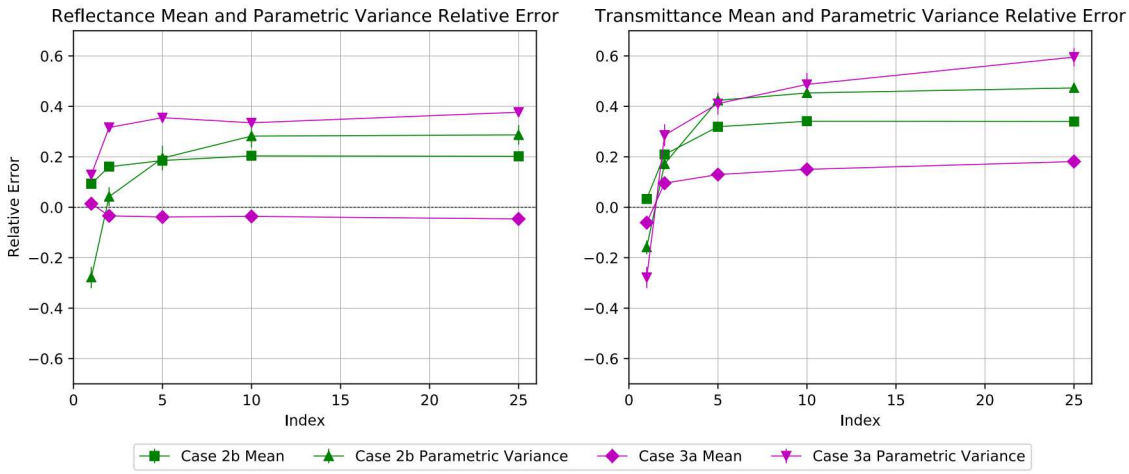

Figure 4: Reflectance and transmittance mean and parametric variance relative error and uncertainty based on index of particle tallied in cohort for Cases 2b and 3a.

Table 5: Reflectance and Transmittance Mean and Parametric Variance Results of Indexed Particle History

	Case	Leakage	Index 1	2	5	10	25
Mean	2b	Ref.	0.263(2)	0.243(2)	0.236(2)	0.231(2)	0.231(2)
		Trans.	0.189(1)	0.155(1)	0.133(1)	0.1292(9)	0.129(1)
	3a	Ref.	0.682(2)	0.715(2)	0.718(2)	0.717(2)	0.724(2)
		Trans.	0.1714(6)	0.1461(6)	0.1406(8)	0.1372(7)	0.1322(8)
Parametric Variance	2b	Ref.	0.0340(9)	0.0255(9)	0.021(1)	0.019(1)	0.019(1)
		Trans.	0.075(1)	0.054(1)	0.037(1)	0.036(1)	0.034(1)
	3a	Ref.	0.0596(8)	0.047(1)	0.044(1)	0.045(1)	0.043(1)
		Trans.	0.039(1)	0.022(1)	0.018(1)	0.016(1)	0.012(1)

media problems from the benchmark suite described in Ref. [1]. Batches of cohorts were used to compute statistical uncertainty on quantities of interest. Results generated using CoPS3 had no statistically significant error. Numerical studies were conducted to assess the accuracy of CoPS2 results as a function of the number of successive particle histories that retain memory of defined material points. Error from this non-errorless 2-point conditional probability function was shown to compound as a function of cohort size strengthening our hypothesis that smaller cohort sizes are more accurate.

In future publications, we hope to improve the efficiency and possibly accuracy of the method using biased Woodcock Tracking [3]. While CoPS has been demonstrated to compute mean values

in multi-dimensional, Markovian-mixed media [5], we plan to implement EVADE in our multi-D implementation of CoPS. We also hope to apply CoPS to non-Markovian and multi-material mixing.

ACKNOWLEDGEMENTS

Sandia National Laboratories is a multimission laboratory managed and operated by National Technology & Engineering Solutions of Sandia, LLC, a wholly owned subsidiary of Honeywell International Inc., for the U.S. Department of Energy's National Nuclear Security Administration under contract DE-NA0003525.

REFERENCES

[1] M. L. Adams, E. W. Larsen, and G. C. Pomraning. "Benchmark results for particle transport in a binary Markov statistical medium." *J Quant Spectrosc and Rad Transfer*, **volume 42**, pp. 253–266 (1989).

[2] G. B. Zimmerman and M. L. Adams. "Algorithms for Monte-Carlo Particle Transport in Binary Statistical Mixtures." *Trans Am Nucl Soc*, **volume 63**, p. 287 (1991).

[3] B. Molnar, G. Tolnai, and D. Legrady. "Variance reduction and optimization strategies in a biased Woodcock particle tracking framework." *Nucl Sci Eng*, **volume 190**, pp. 56–72 (2018).

[4] E. H. Vu and A. J. Olson. "Conditional Point Sampling: A novel Monte Carlo method for radiation transport in stochastic media." *Trans Am Nucl Soc*, **volume 120** (2019).

[5] A. J. Olson and E. H. Vu. "An Extension of Conditional Point Sampling to Multi-dimensional Transport." In *M&C2019*. Portland, OR (2019).

[6] A. J. Olson and B. C. Franke. "An optimal-cost Monte Carlo approach to stochastic media transport calculations." *Trans Am Nucl Soc*, **volume 118** (2018).

[7] S. D. Pautz, B. C. Franke, A. K. Prinja, and A. J. Olson. "Solution of stochastic media transport problems using a numerical quadrature-based method." In *M&C 2013*. Sun Valley, ID (2013).

[8] P. Switzer. "A random set process in the plane with a Markovian property." *Annals of Mathematical Statistics*, **volume 36**, pp. 1859–1863 (1965).

[9] A. J. Olson. "Calculation of parametric variance using variance deconvolution." *Trans Am Nucl Soc*, **volume 120** (2019).